

EVOLUTION OF SUNSPOTS BASED ON VECTOR MAGNETOGRAM AND $H\beta$ FILTERGRAM OBSERVATION

LEE, SANG WOO, YUN, HONG SIK

Department of Astronomy, Seoul National University, Seoul 151-742

AND

MOON, YONG JAE

Bohyunsan Optical Astronomy Observatory, Jachan Post Office PO Box #1, Youngchun, Kyungbook, Korea

AND

WANG, JIA LONG

Beijing Astronomical Observatory, Beijing 100080, China

(Received March Feb. 12, 1996; Accepted Mar. 8, 1996)

ABSTRACT

We have analyzed vector magnetograms and $H\beta$ filtergrams of two sunspot groups, one in a growing phase and the other in a decaying phase. In this study, the temporal evolution of their magnetic morphology has been investigated in association with solar activity. The morphological variations of the growing and decaying phase of these sunspots revealed in detail the coalescence of small spots into a large spot and the fragmentation of a large spot into many small spots, respectively. Numerous small flares were detected in the spot group during the decaying phase. This seems to be intimately associated with the shearing motions of many spots with different polarities created by fragmentation of a large sunspot. The magnetic flux and the average shear angle are found to be substantially reduced during the decaying phase, especially in the course of the flarings. This implies that the decaying phase of the sunspot is, to some degree, involved with magnetic field cancellation. The growi

ng spot group has not shown any large activities, but numerous small spots have grown into a typical bipolar sunspot.

Key Words : sunspot evolution, solar activity, magnetic shear

I. INTRODUCTION

As summarized in Zwaan (1992), the sunspot undergoes its own morphological evolution during the course of the lifetime. Sunspots grow from small pores into a large spot by coalescence from many small magnetic patches and after some period they decay by fragmentation into many smaller spots. In some cases, such an evolutionary characteristics is intimately associated with the formation of an active region, leading eventually to active solar phenomena such as solar flares. Especially during the decaying phase, a lot of small fragmented spots with different polarities makes the field structure very complex, which often causes violent activities.

In this study we have taken two spot groups, one in the growing phase and the other in the decaying phase of sunspot evolution to examine their morphological changes with time. A set of vector magnetograms and $H\beta$ filtergrams has been taken with a vector magnetograph at Huairou Solar Observing Station of Beijing Astronomical Observatory to perform such a study. In addition to the morphological examination, simple quantitative studies have been made on the change of magnetic fluxes and magnetic shears for these two sunspot groups. In Section II, we briefly describe our observation and data reduction. Then, we present the results of our analysis in Section III and summarize the results in Section IV.

II. OBSERVATION and DATA REDUCTION

The photospheric vector magnetogram and $H\beta$ filtergram of two sunspot groups have been taken with a vector magnetograph of Huairou Solar Observing Station of Beijing Astronomical Observatory. The first spot group (Huairou 91234) was observed from November 10 to 17, 1991 and the second spot group (Huairou 91176), from September 7 to 13, 1991. During the observations the first spot group moved from S12.4 E59.2 to S15.1 W29.2 and the second spot group, from S14.3 E25.7 to S14.3 W49.6. The photospheric vector magnetogram was taken in FeI 5324Å line together with the $H\beta$ filtergram to see activities in the chromospheric level. The CCD camera has 512×512 pixels and the image scale per pixel is $0.''67 \times 0.''47$. The observed data has a spatial resolution of $2'' \times 1.''88$, since the data have been averaged over 3×4 pixels.

The longitudinal and transverse components of the photospheric magnetic field are obtained from the observed Stokes parameters through

$$B_l = C_l(V/I)$$

$$B_t = C_t[(Q/I)^2 + (U/I)^2]^{1/4},$$

where C_l and C_t are the field calibration factors for each component. These equations have been used to do the calibration of the magnetograms at Huairou Observing Station.

When the longitudinal field configuration is obtained from the magnetogram observation, the spatial distribution of positive and negative poles is determined so that the direction of the longitudinal field is readily found. The direction of the transverse field, however, cannot be determined directly from the magnetogram, since only the plane of linear polarization is determined from the observation. In order to resolve the problem (180° ambiguity problem), we have adopted two methods, namely the *potential method* and the *charge method*. The *potential method* is to determine the direction of the observed transverse field by taking the direction in which the observed transverse field meets the calculated transverse *potential field* with an angle less than 90° . This method has a weakness in which it cannot effectively describe highly sheared local fields, when the global distribution is dealt. In this case the *charge method* is more effective.

The *charge method* assumes a magnetic charge with strength B at each pixel on the magnetogram. To determine the transverse direction, a unit test charge is introduced at a given point. The direction of the observed transverse field is then determined by taking the direction which satisfies the condition

$$\vec{F}_c \cdot \vec{B}_t > 0,$$

where \vec{F}_c is the net Coulomb force felt by the test charge due to nearby charges within $10'' \sim 20''$ and \vec{B}_t is the observed transverse field. Since we confine our interest to a limited region (within $10'' \sim 20''$), this method is very effective for studying the morphology of strong magnetic shear.

The projection effect of the observed magnetic field configuration has been corrected prior to analysis, for which we have made use of the transformation code developed by Tong-Jiang, Wang. Unfortunately this code does not work well for the magnetograms obtained far from the disk center. Therefore, in the present study only the magnetograms observed near the disk center have been taken for analysis.

III. RESULTS

(a) The Decaying Sunspot: Huairou 91234

Fig. 1(a) shows the monochromatic images of a decaying sunspot, Huairou 91234 taken in FeI 5324Å line for 8 consecutive days. The corresponding magnetograms are shown in Fig. 1(b), which describes the global image-plane magnetic field of this region. On November 10, 1991, it comprised a positive spot with $R \sim 15000\text{km}$ and two smaller spots ($R \sim 8000\text{km}$) of a positive and a negative polarity within one penumbra. Within a couple of days, this spot group underwent fragmentation through a series of magnetic flux tube separation. Here we may note that on

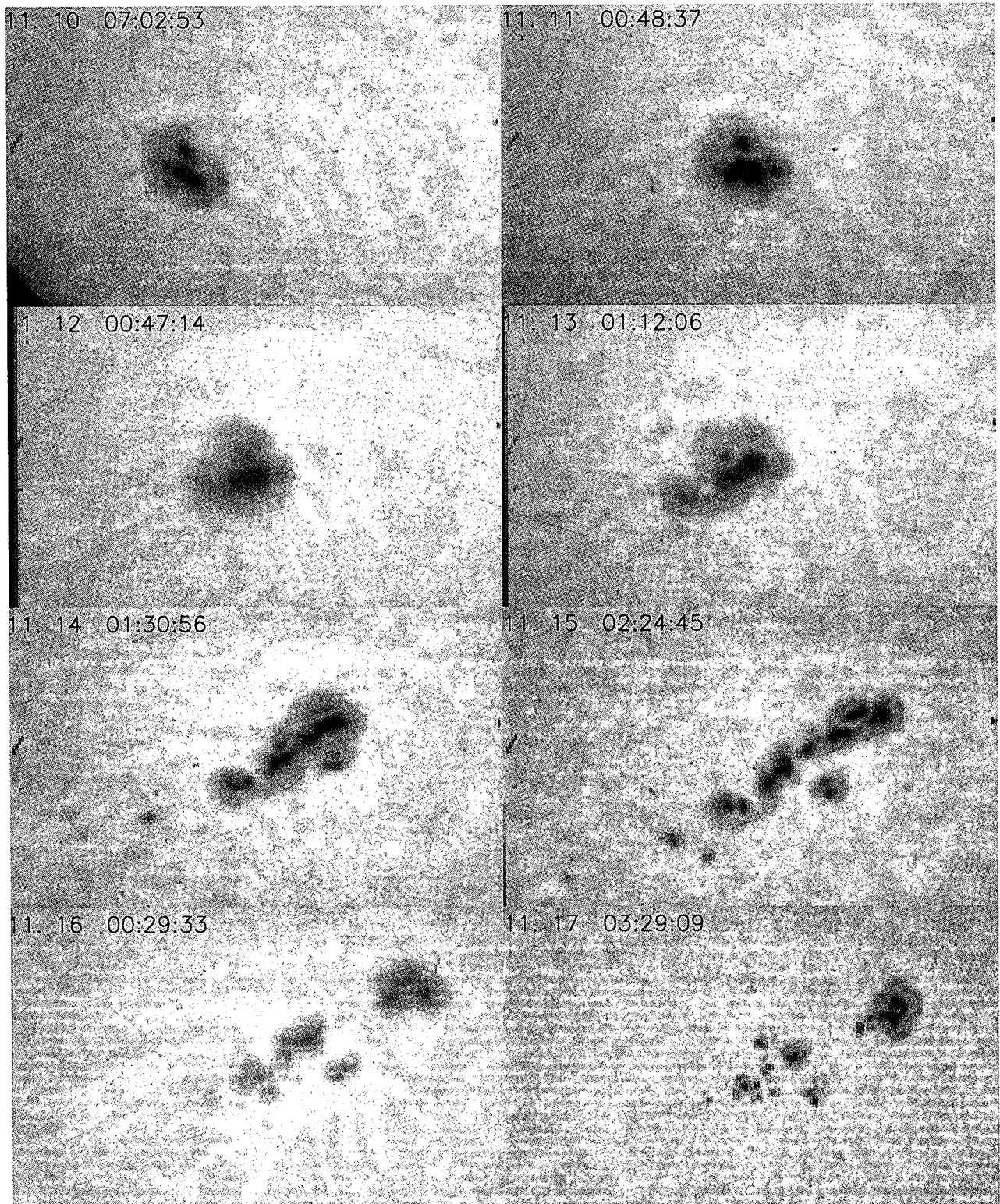


Fig. 1(a). The monochromatic images of the spot Huairou 91234 taken in FeI 5324Å during the 8 consecutive days' observation. The field of view is 5'.7×4'.0.

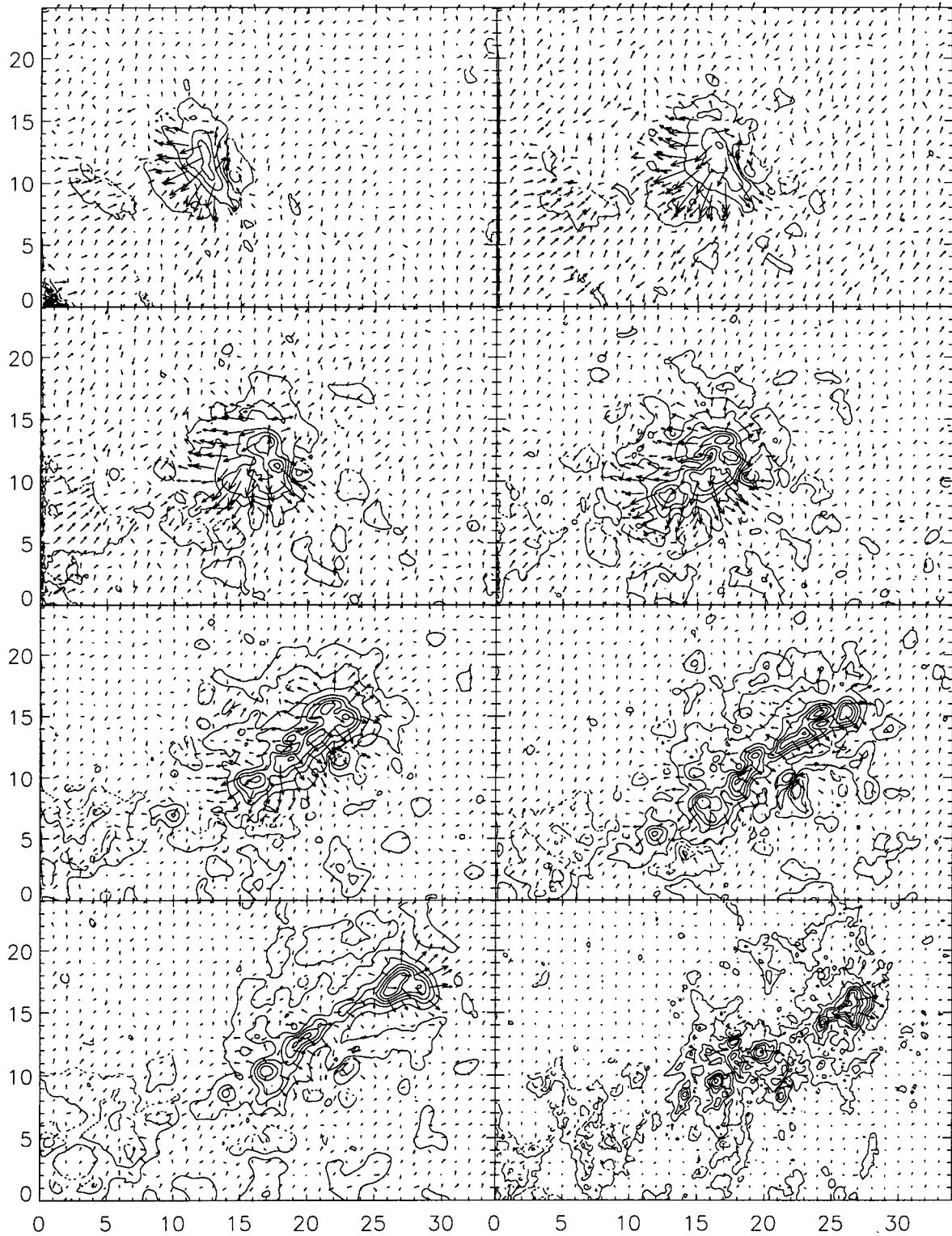


Fig. 1(b). The image-plane vector magnetograms of the spot Huairou 91234 taken in FeI 5324Å during the 8 consecutive days' observation. The field of view is $5'.7 \times 4'.0$. The solid contour lines refer to the longitudinal fields with the positive polarity and the dotted ones with the negative polarity. The length and the direction of arrows refer to the strength and the direction of the transverse field.

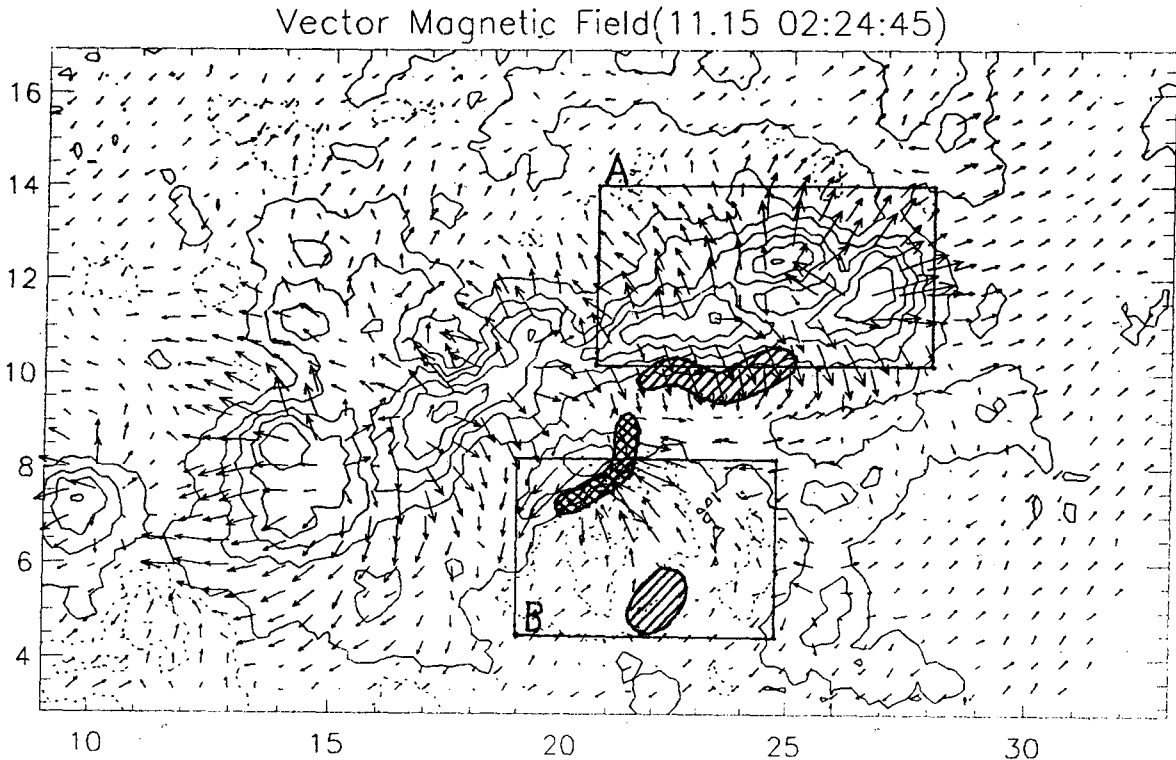


Fig. 2. The magnified picture of the heliographic magnetogram (obtained by correcting for the projection effect of the image-plane magnetogram in Fig. 1(b)) of Huairou 91234 at 02:24:45UT on Nov. 15, 1991. The *charge method* (Wang 1993) was adopted to obtain this magnetogram. The field of view is about $4'.0 \times 2'.3$. The hatched regions refer to the flare kernels observed in $H\beta$ and the cross-hatched region refers to the HXR brightening point observed by Yokoh. The box A is a selected region with the positive polarity and the box B with the negative polarity, where flares have occurred.

November 13 it has been fragmented into several small positive spots ($R=3000\sim 8000\text{km}$) and a negative spot with $R\sim 3000\text{km}$. Such a fragmentation process was most active in November 14 and 15 and the rate of the magnetic tube separation is found to be about 0.4km/s .

This spot group turned out to be a flare producing active region NOAA6919, in which many flares occurred between November 15 and 16. It has a complicated field structure due to many spots gathered in a relatively small area. Small-scale flares were detected at 07:06 on November 15 and 04:48, 06:24 on November 16 during this observation. A large flare, classified as X1.5, was also detected by Yokoh at 22:34 on November 15 (Canfield *et al.* 1992). Fig. 2 shows the heliographic vector magnetogram taken at 02:24:45 on November 15, which has been corrected for the projection effect. The hatched region corresponds to the flare kernel observed in $H\beta$ at 07:08:05 in this observation and the cross-hatched region is the HXR (23–33 keV) brightening point observed by Yokoh at 22:37:32 on November 15. The site of HXR emission corresponds to the footpoint of a flaring loop where the particles accelerated from the loop top penetrate along the field line down to the lower denser layer, interacting with the ambient medium to induce the thermal heating. These flares seem to be caused by a strong magnetic shear due to proper motions of individual magnetic poles, noting that the transverse field lines near the magnetically neutral area lie along the polarity switching inversion line, which is a typical field configuration prior to the flare occurrence. Such a sheared field structure is seen in the boxed area A of Fig. 2.

To quantitatively describe the influence of flares on sunspot evolution, the temporal variation of magnetic flux has been estimated by spatially integrating the longitudinal components of the field in a specified area on the magnetogram. If the photospheric surface is taken to be xy plane, the flux is calculated by

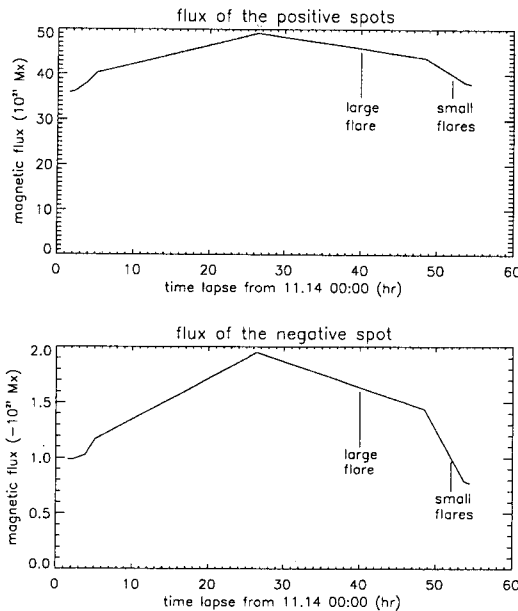


Fig. 3. The temporal variation of the estimated magnetic fluxes.

$$Flux = \int_{\Delta x} \int_{\Delta y} B_z dx dy \quad (Mx)$$

In this study, we have focused on a small positive spot group in the box A and a negative spot in the box B in Fig. 2. In estimating the magnetic flux in the positive spot region (box A), we avoided the parts of the region with the negative polarity and vice versa in the negative spot region (box B). Fig. 3 shows the resulting temporal variations of the magnetic flux in A and B regions. As can be seen from the figures, the measured flux increases continuously throughout November 14 and the early part of November 15 and then it declines steadily for the most of November 15 and 16, during which period the flares have occurred actively. This result implies that flare occurrence is closely associated with the magnetic field cancellation.

We have also considered the degree of the magnetic shear by estimating the magnetic shear angle. Flares usually occur in magnetically highly sheared regions because such a region is in an energy state higher than that of the potential field. When a flare occurs, the accumulated magnetic energy is released explosively. After the flare, we expect that the overall magnetic shear of this region is substantially relaxed. In the present study we define a direction of a magnetic field at a given point on the magnetogram as

$$\tan\theta = B_y/B_x, \quad \tan\theta_p = B_{yp}/B_{xp}$$

where B_x , B_y are the observed field components and B_{xp} , B_{yp} are the corresponding potential field components. Therefore, the shear angle at a given point can be measured by $\theta - \theta_p$. On the magnetograms, the transverse field components usually have noises and irregularities especially when the magnetic field with either small $B_t (= (B_x^2 + B_y^2)^{1/2})$ or large B_t is preferentially considered. Accordingly, in the present work we defined an average shear angle by taking a B_t -weighted spatial mean for the measured shear angle $\theta - \theta_p$ at each point over the whole region on the magnetogram as

$$\theta_a = \frac{\sum B_t^n (\theta - \theta_p)}{\sum B_t^n}.$$

As we increase the value of n in this equation, the field lines with larger B_t are preferentially considered. Hence, the value of n should be taken sufficiently large in order to reduce the influence of the noise and irregularity of the field lines when B_t is small. Table 1 shows the temporal variations of the estimated shear angle θ_a around

Table 1. Temporal variations of the average shear angle.

date / n	2	3	4	5	6	7	8
11. 15 02:24:45	37.2	30.9	27.4	24.9	23.0	21.2	19.6
11. 16 00:29:33	35.5	27.7	23.2	20.0	17.5	15.5	13.9
11. 16 05:40:28	31.2	22.8	19.0	16.8	15.3	14.0	12.9

the above-mentioned flares with n , where we have considered values of n ranging from 2 to 8. It is noted that θ_a decreased after the flare occurrence. The rate of decrease in the shear angle is higher around the time of the large X1.5 X-ray appearance, which indicates that the rate becomes larger for bigger flares.

(b) The Growing Sunspot: Huairou 91176

The sunspot group Huairou 91176 represents a growing phase of the sunspot evolution. As can be seen in Fig. 4, initially it comprised three negative spots with $R=3000\sim 5000\text{km}$ and a few small pores with $R=1000\sim 2000\text{km}$. One positive pore among them grew into a spot with $R\sim 8000\text{km}$ in a day and then absorbed continuously small adjacent positive pores to become a simple rounded spot with $R\sim 12000\text{km}$ on September 9. The three negative spots coalesced into a large spot with $R\sim 10000\text{km}$ in 4~5 days. Eventually, they evolved into a large bipolar spot on September 11. Such an evolutionary characteristics is in agreement with the coalescence picture of sunspot evolution (Zwaan 1992).

Although there were no notable activities in this region, a small local brightening in $H\beta$ was detected on September 8 during the course of the sunspot growth. Fig. 5 shows a vector magnetogram taken at 03:29:10 on September 8, where one positive and two negative pores are seen in the box. The hatched area located near the negative pores refers to the $H\beta$ brightening point appeared at 03:38:07. It seems that these pores form a small magnetic loop, interacting with the large pre-existing magnetic loop. This phenomena is consistent with the cancelling flux model described in Rust et al. (1994). In this model two magnetic loops with opposite polarity approach each other to induce magnetic reconnection (see Fig. 5 in Rust et al. (1994)). In this respect, it is interesting to note that the positive pore forming a small loop has disappeared on September 9, as seen from Fig. 4. This implies that the flare occurrence causes a cancellation of the pre-existing magnetic field.

As done in Huairou 91234, the magnetic flux variation has been also estimated for this spot group to probe its evolutionary characteristics quantitatively. The calculation has been performed on the positive spot which has grown rapidly between September 8 and 9 together with the three negative spots which have grown rather gradually. As seen in Table 2, the the rapid increase in magnetic flux is noted between September 8 and 9, during which time these spots were merged and abruptly developed into a large spot on September 11 (see Fig. 4). After the rapid development, the flux of the three negative spots remains almost unchanged but with a slight decrease in the flux of the positive spot. This spot group is a typical example for the formation of a bipolar sunspot.

IV. SUMMARY

We have examined the morphological evolution of two sunspot groups, one in the growing phase (HR91176) and the other in the decaying phase (HR91234). Their photospheric vector magnetogram and $H\beta$ filtergram have been taken with a vector magnetograph at Huairou Solar Observing Station of Beijing Astronomical Observatory. Their temporal variation of the magnetic field distribution, magnetic flux and average shear angle have been estimated for quantitative analysis. The important findings emerging from the present analysis are as follows.

(1) The decaying sunspot group HR91234 underwent the fragmentation rather rapidly within a few days through the magnetic tube separation.

(2) Numerous small flares detected in the decaying phase of the sunspot group are intimately associated with the shearing motions of many small spots with different polarities created by the fragmentation of the larger spot.

(3) After the flare, the overall magnetic shear and the magnetic flux in the flare region have been substantially

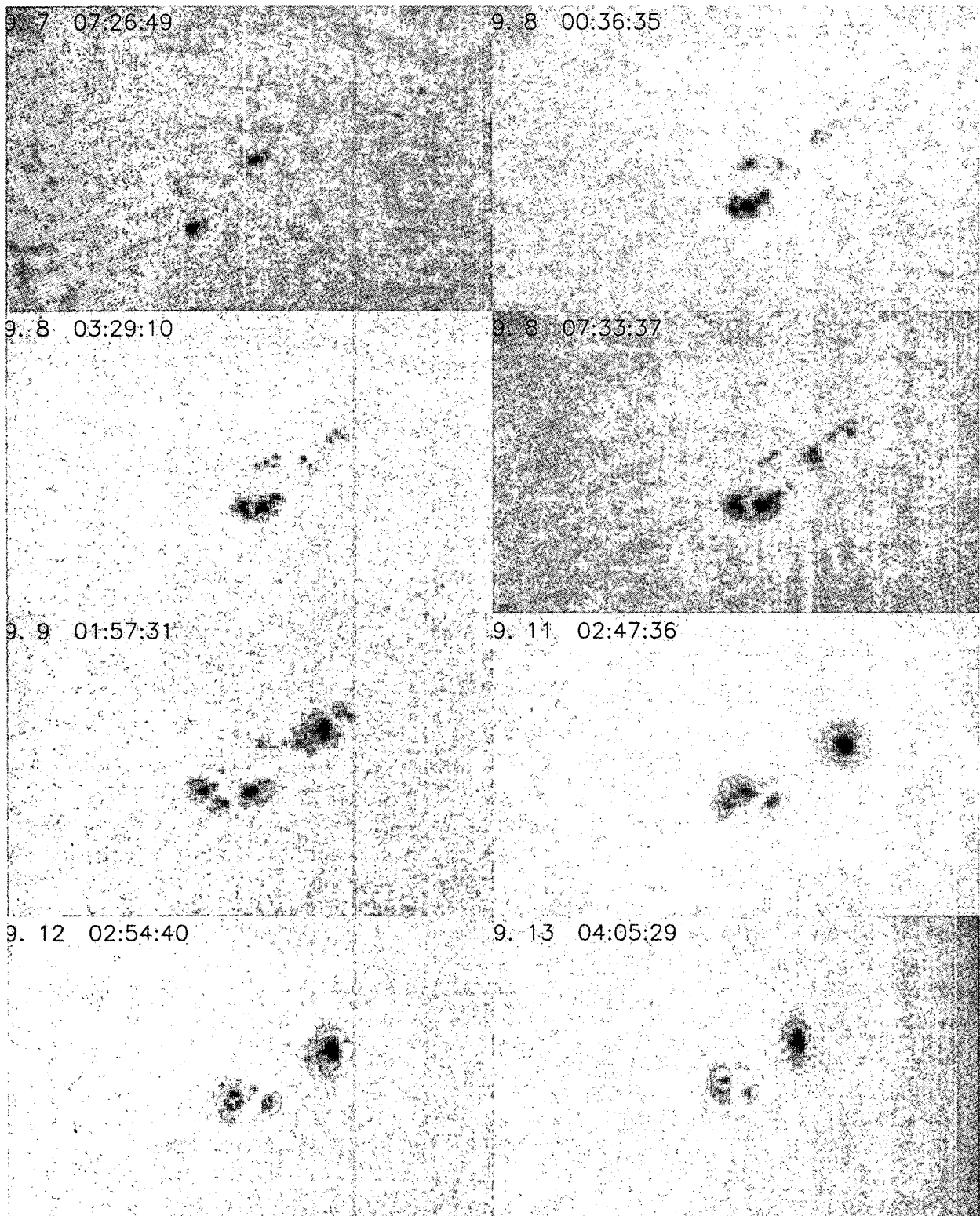


Fig. 4(a). The monochromatic images of the spot Huairou 91176 taken in FeI 5324Å during the 7 consecutive days' observation. The field of view is 5'.7×4'.0.

Table 2. Temporal variations of the magnetic fluxes.

date	flux of the positive pole (10^{21} Mx)	flux of the negative pole (10^{21} Mx)
9. 8 00:36:35	4.51	-3.90
9. 8 03:29:10	4.57	-4.77
9. 9 01:57:31	13.05	-10.00
9. 11 02:47:36	9.66	-10.33

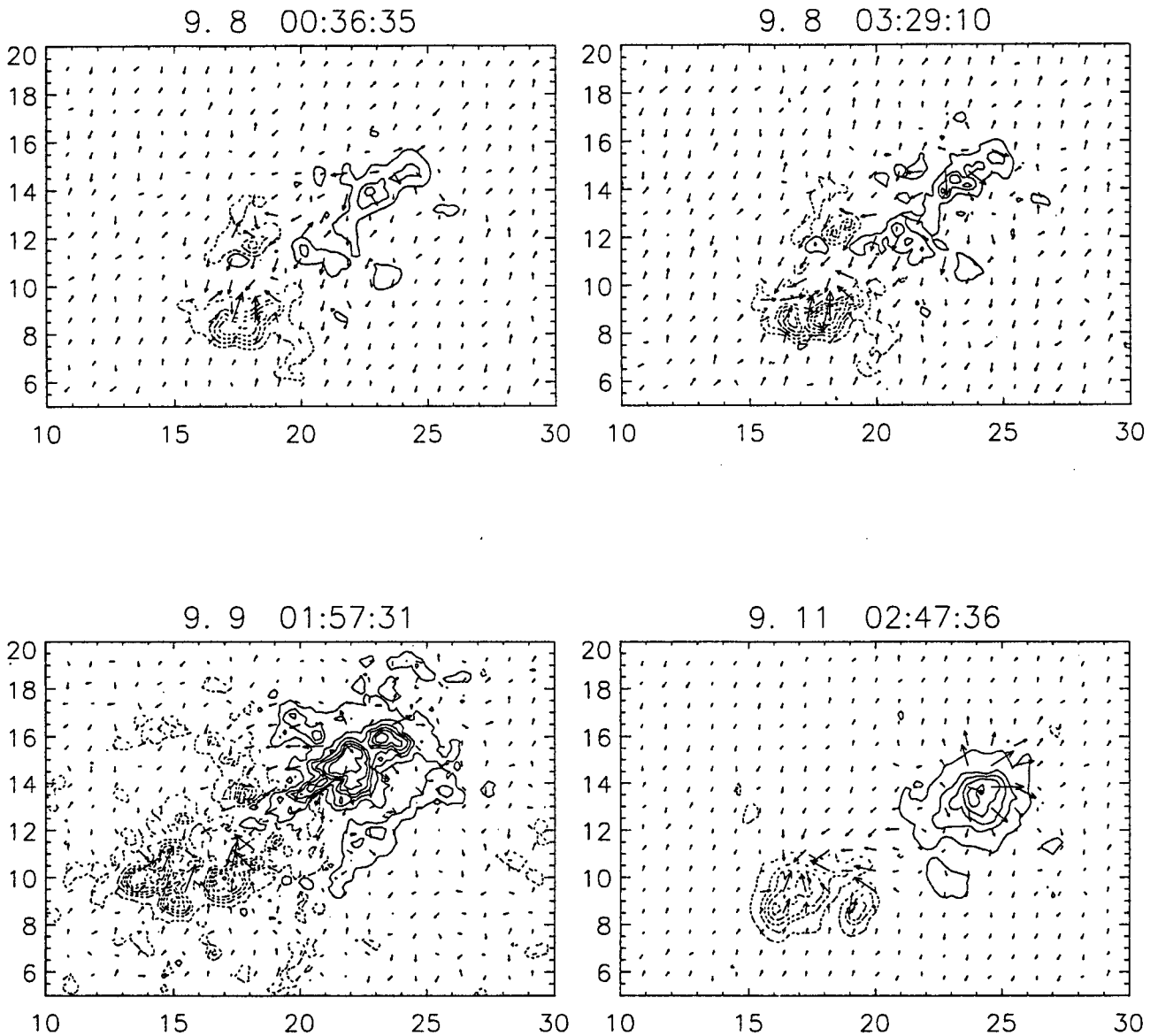


Fig. 4(b). The image-plane (uncorrected) vector magnetograms of the spot Huairou 91176 taken in FeI 5324Å during the 7 consecutive days' observation. The field of view is $3'.4 \times 2'.5$.

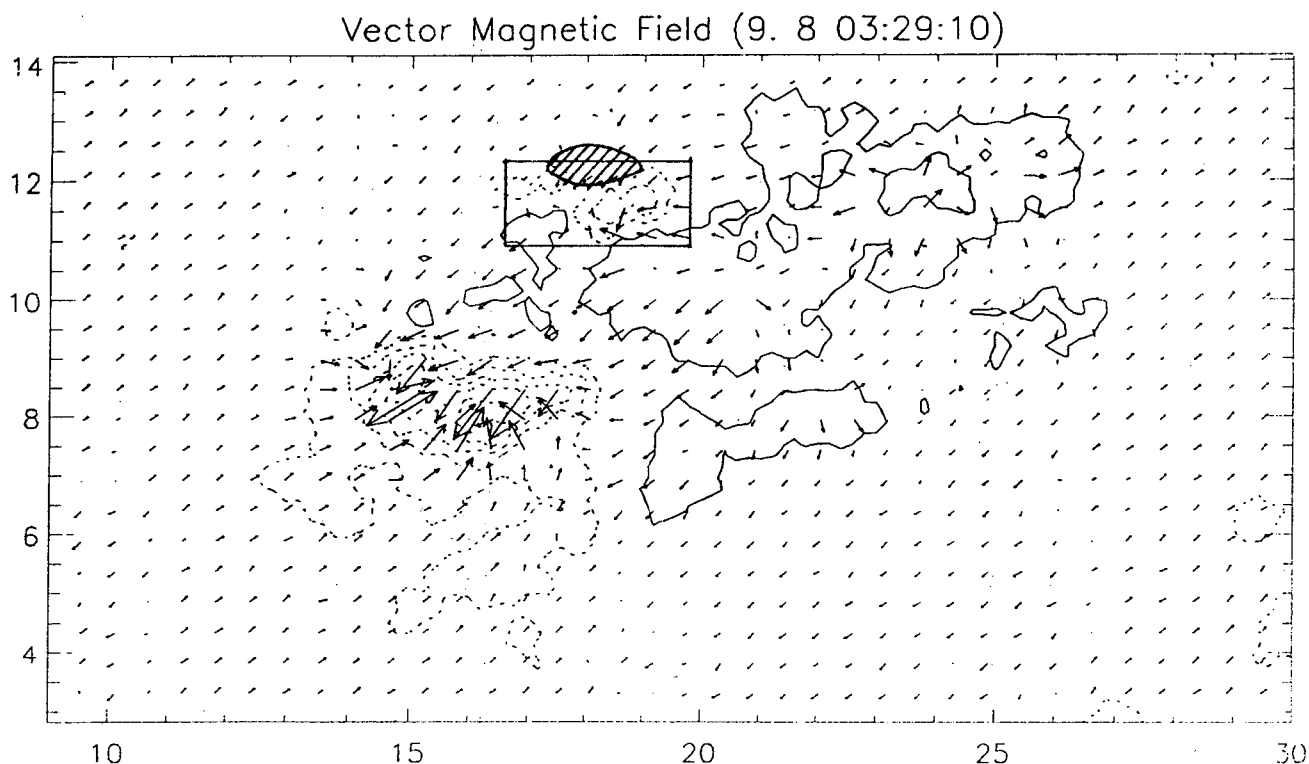


Fig. 5. The magnified picture of the heliographic (corrected) magnetogram (obtained by correcting the image-plane magnetogram in Fig. 4(b) for the projection effect) of Huairou 91176 at 03:29:10UT on Set. 8, 1991. The charge method (Wang 1993) was adopted to obtain this magnetogram. The field of view is about $3'.5 \times 1'.8$.

reduced. This strongly suggests that the decaying phase sunspot is involved with the magnetic cancellation.

(4) The growing sunspot group HR91176 comprising three small spot with the negative polarity coalesced into a large spot within a couple of days, during which time the magnetic flux steadily increased monotonically. After the full development, the flux remained almost unchanged.

(5) A local $H\beta$ brightening observed in the growing spot group appears to be caused by a small magnetic loop formed by the two negative pores and one positive pore, which interacted with the large pre-existing magnetic loop. This is consistent with the flux cancellation model suggested by Rust et al. (1994).

ACKNOWLEDGEMENT

We wish to thank Prof. G., Ai, Dr. H., Zhang and his colleagues for their hospitality given to us during the two-month stay at Huairou Solar Observing Station of Beijing Astronomical Observatory in the summer of 1994. The present work is supported by the Basic Science Research Institute Program, Ministry of Education, 1995 (BSRI-95-5408) and in part by KOSEF and NSFC for the Korea-China Cooperative Science Program (1993–1995).

REFERENCES

- Canfield, R. C., Hudson, H. S., Leka, K. D., Mickey, D. L., Metcalf, T. R., Wulser, J. -P., Acton, L. W., Strong K. T., Kosugi, T., Sakao, T., Tsuneta, S., Culhane, J. L., Phillips, A., & Fludra, A. 1992, *P.A.S.J.*, **44**, L111.
- Rust, D. M., Sakurai, T., Gaizauskas, V., Hoffmann, A., Martin, S. M., Priest, E. R. & Wang, J. 1994, *Solar Phys.*, **153**, 1.
- Wang, J. 1993, *A.S.P.C.S.*, **46**, 425.
- Zwaan, C., 1992, *Sunspots: Theory and Observation*, p75